N91-10476

CIRRUS CLOUD PROPERTIES DERIVED FROM COINCIDENT GOES AND LIDAR DATA DURING THE 1986 FIRE CIRRUS INTENSIVE FIELD OBSERVATIONS

Patrick Minnis and Jose M. Alvarez
Atmospheric Sciences Division, NASA Langley Research Center
Hampton, Virginia 23665-5225

David F. Young and Patrick W. Heck
Aerospace Technologies Division, Planning Research Corporation
Hampton, Virginia 23666
and
Kenneth Sassen
Department of Meteorology, University of Utah
Salt Lake City, Utah 84112

1. Introduction

One of the main difficulties in detecting cirrus clouds and determining their correct altitude using satellite measurements is their non-blackness. In the present algorithm (Rossow et al., 1985) used by the International Satellite Cloud Climatology Project (ISCCP), the cirrus cloud emissivity is estimated from the derived cloud reflectance using a theoretical model relating visible (VIS, 0.65 μm) optical depth to infrared (IR, 10.5 μm) emissivity. At this time, it is unknown how accurate this approach is or how the derived cloud altitude relates to the physical properties of the cloud. The First ISCCP Regional Experiment (FIRE) presents unique opportunities for determining how the observed radiances depend on the cloud properties. During the FIRE Cirrus Intensive Field Observations (IFO, see Starr, 1987), time series of cloud thickness, height, and relative optical densities were measured from several surface-based lidars. Cloud microphysics and radiances at various wavelengths were also measured simultaneously over these sites from aircraft at specific times during the IFO (October 19 - November 2, 1986). Satellite-observed radiances taken simultaneously can be matched with these data to determine their relationships to the cirrus characteristics. In this paper, a first step is taken toward relating all of these variables to the satellite observations. Lidar-derived cloud heights are used to determine cloud temperatures which are used to estimate cloud emissivities from the satellite IR radiances. These results are then correlated to the observed VIS reflectances for various solar zenith angles.

2. Data and approach

Half-hourly 1-km VIS and 4-km IR radiances from the Geostationary Operational Environmental Satellite (GOES) taken during the IFO are used to determine cloud reflectance and effective blackbody temperatures over two sites, Ft. McCoy and Wausau, Wisconsin. The VIS counts are converted to reflectances using the calibration parameters given by Whitlock (1987). All of the data found within 0.35° longitude and 0.25° latitude of the ground sites are assumed to be representative of the radiances directly above the ground site during a 30-minute interval. Thus, spatial variations near the station replace the time variations in the clouds as they advect over the station. This assumption also minimizes the effects of navigational errors.

In this initial study it is assumed that the pixels are entirely clear or cloud-filled. Therefore, given an equivalent blackbody, clear-sky

temperature, TS, a measured IR temperature, T, and a cloud temperature, TC, it is possible to estimate the cloud emissivity as

$$\epsilon = (B(T) - B(TS))/(B(TC)-B(TS)),$$

where B represents the Planck blackbody function. This simple model treats the cloud as a homogeneous mass radiating at some effective temperature TC. The dependence of ϵ on viewing zenith angle, VZ, is ignored here because all of the measurements are taken at $51^0 < VZ < 52^0$. Since the VIS data are discretized to 6 bits, there are only a few values of reflectance, ρ, which will be observed at a given hour. In order to determine ϵ as a function of ρ, the emissivities measured for some given value of ρ are averaged to yield a single value for each reflectance value. This averaging process tends to smooth out some of the inhomogeneities found in real clouds.

A first guess value of TS was taken from the time series results for clear-sky temperature derived by Heck et al. (1988). This value was reset to the highest observed temperature over the site whenever a negative average emissivity was found. Cloud temperature was determined in the following manner. First, a density center for the cloud in terms of altitude was estimated from time series plots of lidar relative backscatter intensities. These intensities were taken by the NASA Langley ground lidar system operating at Ft. McCoy (Alvarez et al., 1988) and by the University of Utah mobile polarization lidar at Wausau (Sassen, 1987). An initial guess of TC was taken from the nearest available radiosonde data using the temperature corresponding to the density center height. This process assumes that this inferred "center of mass" is the radiating core of the cloud. Whenever any of the derived emissivities exceeded unity, TC was reset to the coldest observed temperature. Underestimates of TC may be detected from a flattening of the emissivity curve long before $\epsilon = 1$.

3. Results and discussion

A plot of the Ft. McCoy lidar returns for 1500 - 2200 UT, Oct. 28, 1986 is shown in Fig. 1 with the selected values of cloud height and TC. In the morning, the cloud altitude was lower and the clouds described as "mackerel" indicative of alto- or cirrocumulus. By 1900 UT, a cirrus deck of variable thickness advected over the area between 8 and 11 km. Before 2030 UT, the clouds were generally described as thin and variable. Between 2030 and 2200 UT, the cloud deck was described as uniform with some "bluish" areas in the clouds. Cloud emissivities over Ft. McCoy for 1500 UT, 1930 UT, and 2100 UT are plotted as functions of VIS reflectances in Fig. 2. These results appear to be consistent with the surface descriptions. At 1500 UT, the points yield a smooth curve indicating a relatively homogeneous cloud deck, while at 1930 UT the values of ϵ do not vary monotonically with ρ, suggesting the presence of some lower-level clouds or partially-filled pixels. The curve for 2100 UT is also relatively smooth.

Some values of ρ in Fig. 2 are actually less than the nominal clear-sky reflectance. Since this occurs for $\epsilon > 0.1$, this phenomenon may be due to either shadowing of a lower part of the cloud by a thick part or due to the transmission properties of the clouds. The 3-km altitude variation in the cells around 2100 UT seen in Fig. 1 indicates that such a shadowing effect is possible for that hour. Additional examination of the pixel maps will help determine the reasons for the decreased reflectances.

Figure 3 shows the emissivities derived from data over both sites for hours 1500 UT and 2130 UT on Oct. 28. The solar zenith angles are about 68^0

at 1500 UT and 78° at 2130 UT. Relative azimuth angles are approximately 130° in both cases. The variation of ϵ with ρ appears to be consistent between the sites but differs from the morning to the afternoon. Emissivity increases rapidly until a value of $\epsilon = 0.8$ is reached in Fig. 3a, then it increases with a decreasing slope. In Fig. 3b, the slope appears to increase gradually up to $\rho = 25\%$, then more rapidly, at least for the Ft. McCoy data. The clouds are 1-2 km higher in the afternoon, but the slope at 2100 UT (Fig. 2c) is very similar to the 1500 UT case. Although there may be enhanced shadowing at 2130 UT, it is not immediately apparent why this large difference occurs.

Emissivities derived over Ft. McCoy on three different days at 2030 UT are given in Fig. 4. Variations in their dependence on VIS reflectance probably result from variations in the cloud microphysics and morphologies. The lidar returns indicate that the clouds are thickest on Oct. 28. On Oct. 27 the clouds are only about 1 km thick with no obvious precipitating cells. All three cloud decks were between 9 and 10 km. The dip in the emissivity at the highest reflectances may correspond to views of the sides of the cirrus clouds. Since these data are taken in a backscattering geometry with a low sun and satellite, the cloud sides would be intercepting and reflecting a considerable fraction of the incident radiation. Viewing of the cloud sides would tend to increase the observed IR radiance since both the top and lower portions of the clouds are seen.

4. Concluding remarks

The analysis of combined satellite and lidar data will help improve our understanding of how to interpret radiances observed over cirrus cloud fields. Examples given here show significant variability in the relationship between VIS reflectance and IR emissivity. Other complicating factors such as shadows, finite cloud geometry, and partially cloud-filled pixels are also apparent in these initial results. The similarities in some of the cases reported here, however, show potential for some empirical modeling. Further study of these and other cases with additional correlative FIRE data will be required to develop parameterizations for interpreting these radiances for cirrus cloud quantification from satellites.

5. References

Alvarez, J. M., M. P. McCormick, J. D. Moore, W. H. Hunt, B. R. Rouse, L. R. Poole, and B. D. Poole, 1988: A Synopsis of Langley Research Center's Lidar Effort for the 1986 FIRE IFO. FIRE Workshop, Vail CO, July 11-15.

Heck, P. W., D. F. Young, P. Minnis, E. F. Harrison, 1988: Cloud Parameters From GOES Visible and Infrared Radiances During the FIRE Cirrus IFO, October 1986. FIRE Workshop, Vail CO, July 11-15.

Rossow, W. B., F. Mosher, E. Kinsella, A. Arking, M. Desbois, E. Harrison, P. Minnis, E. Ruprecht, G. Seze, C. Simmer, and E. Smith, 1985: ISCCP Cloud Algorithm Intercomparison. J Clim. Appl. Meteor., 24, 877-903.

Sassen, K., 1987: The Structure of Cirrus Clouds. FIRE Experiment Team Workshop, Linithicum, MD, Nov. 9-12, 91-104.

Starr, D. O'C., 1987: A Cirrus-Cloud Experiment: Intensive Field Observations Planned for FIRE. Bull. Amer. Meteor. Soc., 68, 119-124.

Whitlock, C.H., 1987: Satellite Calibration Values for the FIRE/SRB Wisconsin Experiment. NASA memo, December 8.

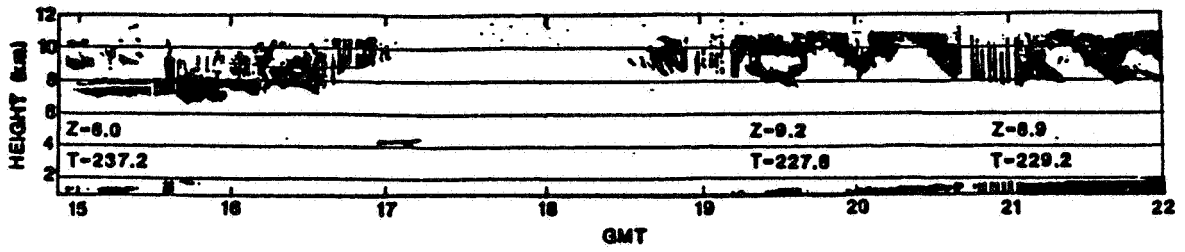

Figure 1. Time series of Ft. McCoy returned lidar power for 1500 UT - 2200 UT, Oct. 28. Estimated height (Z) and temperature (T) for the "center of mass" of the cirrus are given for 1500, 1930, and 2100 UT

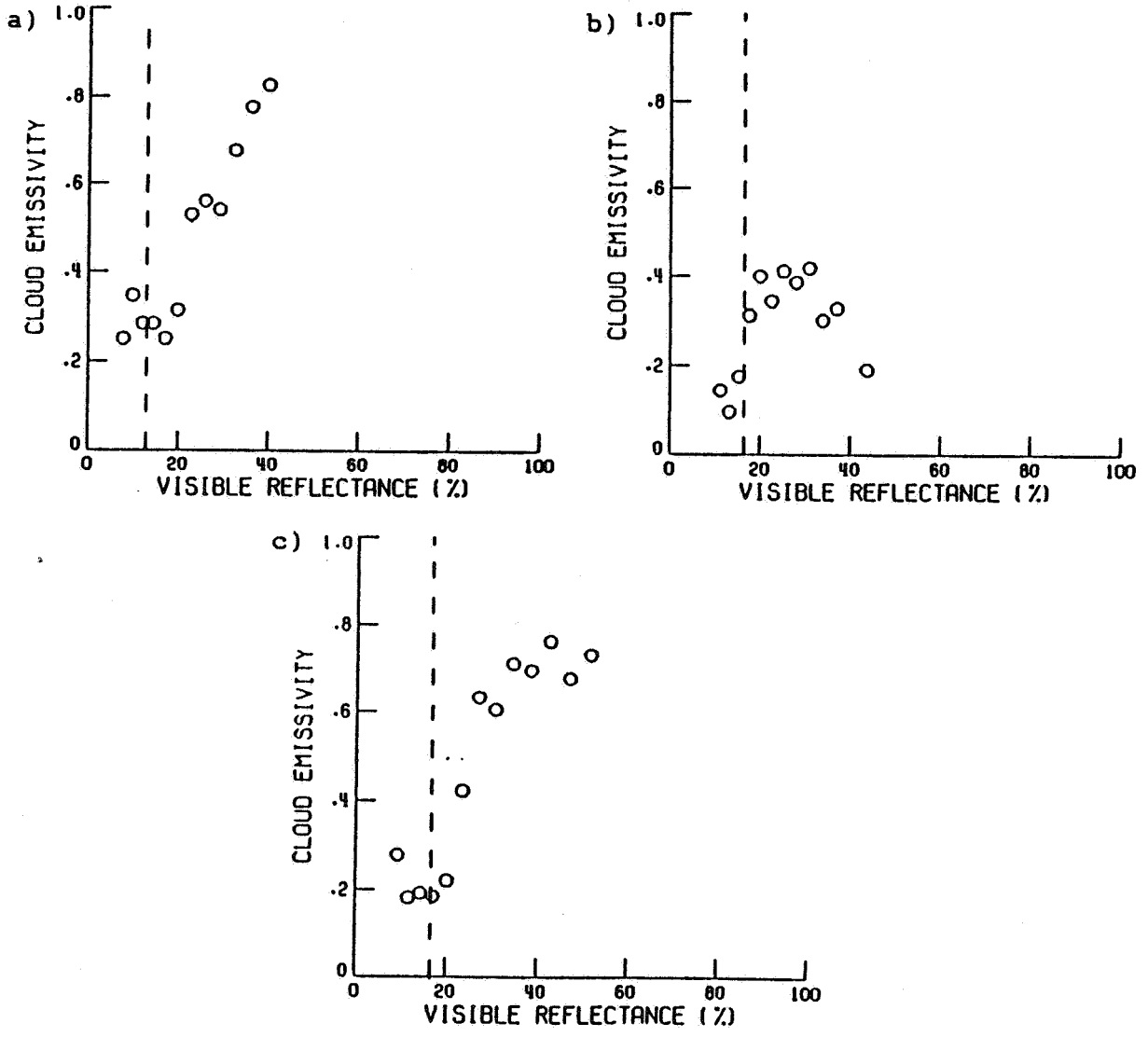

Figure 2. Variation of cirrus cloud emissivity with visible reflectance for a) 1500 UT, b) 1930 UT, and c) 2100 UT for Oct. 28. The dashed line represents the nominal clear-sky reflectance

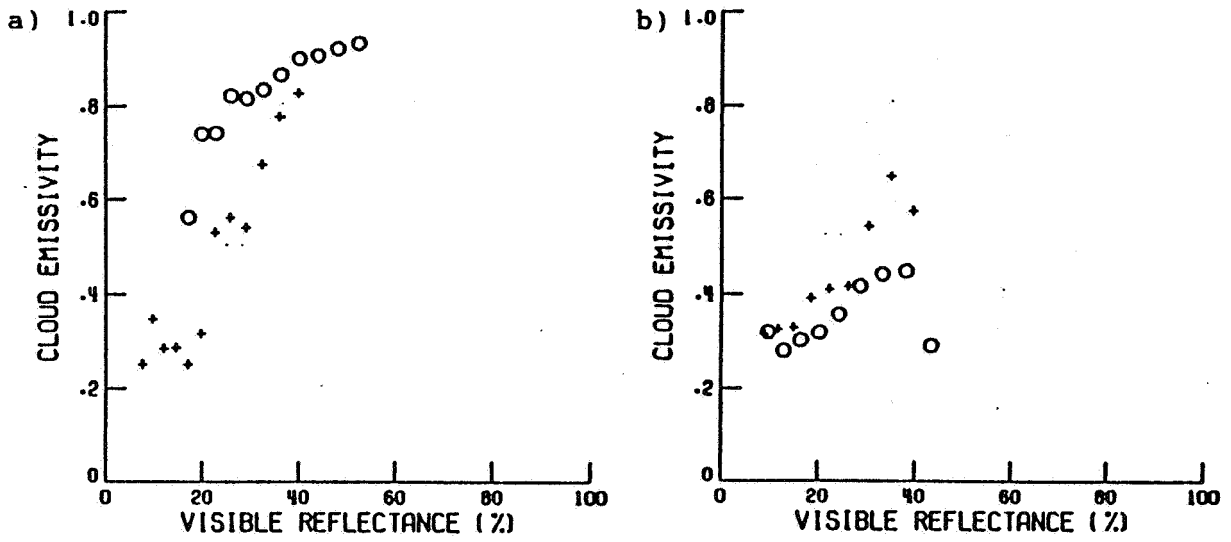

Figure 3. Comparison of Wausau (O) and Ft. McCoy (+) emissivity curves for a) 1500 UT and b) 2130 UT, Oct. 28.

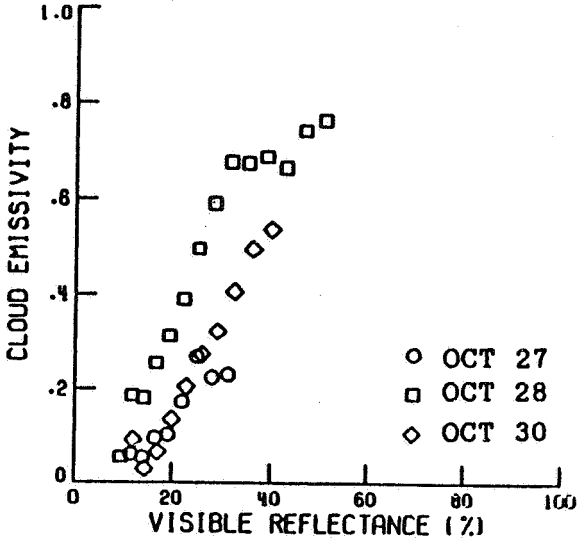

Figure 4. Comparison of Ft. McCoy emissivity curves for Oct. 27, 28, and 30.